Available online at www.sciencedirect.com
ScienceDirect
Ceramics International 35 (2009) 1051–1055
CERAMICS INTERNATIONAL
www.elsevier.com/locate/ceramint

Effects of MO (M=Ba, Mg, Ca) on the crystallization of B_2O_3–Al_2O_3–SiO_2 glass-ceramics

Tao Sun [a], Hanning Xiao [a,b,*], Yin Cheng [b], Huabin Liu [a]

[a] College of Materials Science and Engineering, Hunan University, Changsha 410082, China
[b] College of Materials Science and Engineering, Changsha University of Science & technology, Changsha 410076, China

Received 6 February 2008; received in revised form 18 February 2008; accepted 24 April 2008
Available online 12 July 2008

Abstract

The effects of MO (M=Ba, Mg, Ca) on the crystallization of B_2O_3–Al_2O_3–SiO_2 glass-ceramics were investigated by means of differential scanning calorimetry (DSC), X-ray diffraction (XRD), scanning electron microscopy (SEM) and dilatometer. MO can effectively facilitate the formation of B_2O_3–Al_2O_3–SiO_2 glass which is influenced by the ratio of B_2O_3/SiO_2, and the crystallization capacity of the glass turns to weaker with the decreasing of B_2O_3/SiO_2 ratio. The main crystal phase is $Al_4B_2O_9$ when the glass is heat-treated at 800 °C, and $Al_4B_2O_9$ phase could transfer into $Al_{18}B_4O_{33}$ with the heat-treated temperature increasing to 1100 °C. The calculation of crystallization activation energy (E) shows that crystallinity follows the order of CaO < MgO < BaO, and the Avrami parameter n is higher than 4, which indicate the crystallization of B_2O_3–Al_2O_3–SiO_2 glass to be bulk nucleation with three-dimensional crystal growth. The addition of MO has evident effects on the main crystalline phase and the morphology of the crystals.

Keywords: D. Alkaline earth oxide; D. B_2O_3–Al_2O_3–SiO_2 glass-ceramics; Crystallization kinetics; Microstructure

1. Introduction

The glass-ceramics in B_2O_3–Al_2O_3–SiO_2 system have aroused considerable interest due to its low thermal expansion coefficient, long chemical durability, superior biocompatibility and high electrical resistivity, etc., which make them potential applications in the fields of electronics, information, mechanical and chemical engineering. A number of studies on crystallization behavior and their properties in B_2O_3–Al_2O_3–SiO_2 glass-ceramics have been carried out. Liu and Wang have studied the relationship between the SiO_2/B_2O_3 mol ratio and thermal expansion coefficient of B_2O_3–Al_2O_3–SiO_2 glasses. They reported that the thermal expansion coefficient decreased and the transformation temperature increased with the increase of the SiO_2/B_2O_3 ratio [1]. Vergano has developed a method for diffusion doping of silicon and germanium semiconductors by the vapor phase transport of B_2O_3 from a solid B_2O_3 source to the silicon semiconductor, wherein the solid B_2O_3 source was B_2O_3–Al_2O_3–SiO_2 glass-ceramics [2]. Hamzawy and ALi explored the B_2O_3–Al_2O_3–SiO_2 system to synthesize boralsilite by sol–gel process, but the crystalline phases were found to be mullite, $Al_4B_2O_9$ and B-mullite ($Al_{18}B_4O_{33}$) rather than a pure crystalline $Al_{16}B_6Si_2O_{37}$ phase [3]. Zheng et al. have investigated the phase separation and the crystallization of glasses based on the B_2O_3–Al_2O_3–SiO_2 system contained CaO [4].

B_2O_3 and SiO_2 are both network-forming oxides, Al_2O_3 is an intermediate oxide [5]. According to the conditions of glass formation, glass bodies in the B_2O_3–Al_2O_3–SiO_2 system are rarely formed. Since Si^{4+} and B^{3+} ions possess rather high field strength; there is a lack of oxygen ions in the structure of the B_2O_3–Al_2O_3–SiO_2 system. So, alkaline earth oxides, which have low field strength are usually introduced in the glass system.

In this paper, the effects of alkaline earth oxides MO (M = Ba, Mg, Ca) as network modifiers on the melting property and crystallization of B_2O_3–Al_2O_3–SiO_2 glass were studied; the thermal expansion coefficient and soften temperature of the glass-ceramics were tested and analyzed.

* Corresponding author at: College of Materials Science and Engineering, Hunan University, Changsha 410082, China. Tel.: +86 731 8822269; fax: +86 731 2617678.
E-mail address: hnxiao@hnu.cn (H. Xiao).

0272-8842/$34.00
doi:10.1016/j.ceramint.2008.04.017

Table 1
Chemical compositions of glass samples (in mol ratio)

Sample	B_2O_3	SiO_2	Al_2O_3	BaO	MgO	CaO
BS1	10	5	3.5	1	–	–
BS2	8	5	3.5	1	–	–
BS3	6	5	3.5	1	–	–
BS4	5	5	3.5	1	–	–
BS5	3	5	3.5	1	–	–
BS4-M	5	5	3.5	–	1	–
BS4-C	5	5	3.5	–	–	1

2. Experiments

The chemical composition of all materials used is presented in Table 1, which was designed according to the phase diagram of B_2O_3–Al_2O_3–SiO_2 system. The compositions of BS series were characterized by fairly similar contents of Al_2O_3, and SiO_2, but they had different B_2O_3/SiO_2 ratios, from 2.0 to 0.6, influencing the rate of crystallization and phase composition of the resulting glass-ceramics. BS4-M and BS4-Cwere gained by replacing composition BaO from BS4 with MgO and CaO, respectively. Reagent-grade raw materials of H_3BO_3, Al_2O_3, SiO_2, $BaCO_3$, $MgCO_3$ and $CaCO_3$ with purities higher than 99 wt% were chosen as starting materials. After mixing uniformly, the batches were melted in the temperature range 1500–1600 °C and the resulting liquid cooled in graphite mould, then transferred to an annealing furnace set at about 550 °C and held for 60 min for annealing before cooling down to room temperature, finally, the glass was cut into small pieces for tests.

The crystallization kinetics of B_2O_3–Al_2O_3–SiO_2 glass were determined by differential scanning calorimetry (DSC) method which was performed by NETZSCH STA409C calorimeter at different heating rates (5, 10, 15 and 20 °C min^{-1}). Crystal phases of reheated samples were analyzed by X-ray diffraction (XRD) using CuKα radiation with a Rigaku D/Max 2550 VB^+ 18 kW equipment. Microstructure of the reheated samples was observed using JSM-6700F scanning electronic microscopy. The thermal expansion coefficient of the crystallized examples was measured using a dilatometer (DIL 402PC, Netzsch, Germany).

3. Theoretical basis

Solid state reactions such as the crystallization glass can be described by the phenomenological Johnson–Mehl–Avrami (JMA) equation [6–8].

$$\chi = 1 - \exp[-(kt)^n] \tag{1}$$

Taking natural logarithms and rearranging Eq. (1)

$$\ln[-\ln(1-\chi)] = n\ln K + n\ln t \tag{2}$$

can be obtained, where χ is the volume fraction crystallized after time t, it can be estimated by the area of crystallization exothermal peak [9], as shown in Fig. 1, χ is the ratio of S_χ/S. n is a dimensionless parameter related to the reaction mechanism [10] shown in Table 2, and k is the reaction rate constant (s^{-1}),

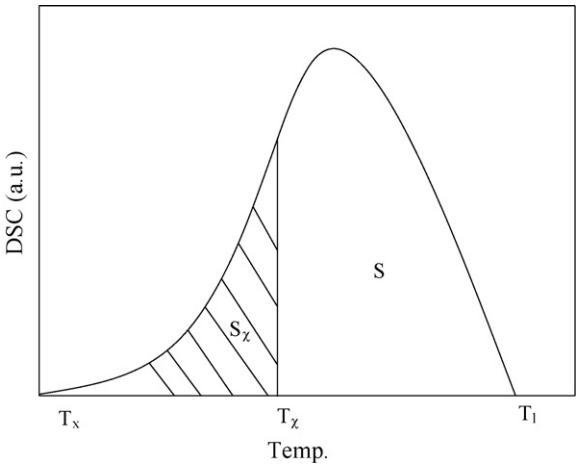

Fig. 1. Estimation of the volume fraction of crystals. T_x and T_l are the onset temperature and end temperature of exothermic peak, respectively; S is the total area of crystallization exothermal peak; S_χ is partial area between T_x and T_l. χ is the ratio of S_χ/S.

Table 2
The values of n for various crystallization mechanisms

Mechanism	n
Bulk crystallization	
Three-dimensional growth	4
Two-dimensional growth	3
One-dimensional growth	2
Surface crystallization	1

whose temperature dependence is generally expressed by the Arrhenius equation.

$$k = V\exp\left(\frac{-E}{RT}\right) \tag{3}$$

or taking natural logarithms

$$\ln K = \ln V - \frac{E}{RT} \tag{4}$$

where V is a frequency factor (s^{-1}), E is the activation energy for crystallization (J mol^{-1}), R is the gas constant (8.314 J mol^{-1}) and T is the absolute temperature (K).

DSC is very effective for determining the kinetic parameters of glass crystallization under non-isothermal conditions [11–13]. The activation energy of crystal growth, E, can be estimated by the Ozawa plot [14]

$$\ln\alpha = -\frac{E}{R}\frac{1}{T_p} + C_1 \tag{5}$$

where C_1 is a constant, α is the heating rate in the DSC, E is the crystallization activation energy, T_p is the temperature of maximum DSC crystallization peak. A plot of $\ln\alpha$ versus $1/T_p$ is expected to be linear. So activation energy, E, can be attained via this expression.

A method which was developed also by Ozawa is used to calculate the n values using the DSC results [6,7]:

$$\ln[-\ln(1-x)] = n\ln k(T - T_0) - n\ln\alpha \tag{6}$$

From Eq. (6)

$$\left.\frac{\mathrm{d}\ln[-\ln(1-x)]}{\mathrm{d}\ln\alpha}\right|_T = -n \quad (7)$$

On this basis, plotting $\ln[-\ln(1-x)]$ versus $\ln\alpha$ yields a straight line with slope equal to n. Here x should be measured at the same temperature from a number of crystallization exotherms obtained at different heating rates.

4. Results and discussion

Composition BS1 turned to opaque during the cooling process, and there were some infusible compositions in BS5; therefore, further studies are carried out only using the samples of BS2, BS3, BS4, BS4-M and BS4-C.

The DSC curves of glass samples at heating rates of 10 °C min^{-1} are shown in Fig. 2. The observed exothermic peak is associated with the crystallization process of the glass, and the exothermic peaks shift to higher temperatures with the decrease in B_2O_3/SiO_2 ratio, which suggests that the increase in B_2O_3 content in the B_2O_3–Al_2O_3–SiO_2 system can improve the crystallization of the glass. To the samples with the same B_2O_3/SiO_2 ratio, the temperature starting crystallization increases in the order of BaO < MgO < CaO. The exothermic peak of the samples is sharp and the integral area is small, indicating the crystallization to be hard, so a strict heat-treated route is needed. Table 3 shows the values of the crystallization peak temperature of DSC experiments of glass samples at different heating rates.

The E values of the glass samples are shown in Table 4, calculated from the slope of $\ln\alpha$ versus $T_p^{-1} \times 10^4$ curves shown in Fig. 3. According to the E value, crystallization capacities of BS series specimens increase with the change in B_2O_3/SiO_2 ratio in the order of 1, 1.2, 1.6, and the crystallization capacities of the samples with the same B_2O_3/SiO_2 ratio increase in the order of CaO < MgO < BaO. The parameter n determined from the slope of $\ln[-\ln(1-x)]$ versus $\ln\alpha$ curves shown in Fig. 4 is also listed in Table 4. The values changed in different samples, but they are all greater than 4 except for sample BS4-C which is 3.7, indicating that the crystallization mechanism of B_2O_3–Al_2O_3–SiO_2 glass with different compositions are caused by bulk nucleation with three-dimensional crystal growth.

Table 3
The crystallization temperature T_p(°C) at different heating rate α of DSC

Sample	α			
	5 °C min^{-1}	10 °C min^{-1}	15 °C min^{-1}	20 °C min^{-1}
BS2	738.1	753.6	762.5	768.3
BS3	747.6	762.5	770.8	778.0
BS4	771.3	785.6	793.9	801.7
BS4-M	785.9	799.7	808.1	814.4
BS4-C	792.8	805.9	814.5	820.9

Table 4
The activation energy E and Avrami parameter n of samples

Sample	E (kJ mol^{-1})	n
BS2	399.5	4.9
BS3	410.1	4.5
BS4	430.6	5.3
BS4-M	466.7	4.5
BS4-C	479.0	3.7

Fig. 5 shows the XRD patterns of sample BS3 heat-treated under different conditions. The sample starts crystallization at about 800 °C, and the crystallization capacity is improved with the increase in temperatures and holding time. The main crystalline phase is $Al_4B_2O_9$ at 800 °C which is orthorhombic structure, and $Al_{18}B_4O_{33}$ phase appeared at 1100 °C, turning to be the predominating crystalline phase with the holding time from 2 to 5 h. The XRD patterns of sample BS4, BS4-M and BS4-C (Fig. 6) indicate that $Al_{18}B_4O_{33}$ is the main crystalline phase in the sample BS4 and BS4-C, but the main crystalline phase in the sample BS4-M is $Al_4B_2O_9$, and cubic B_2O_3 phase is detected. According to the results of precious studies [15,16], $Al_4B_2O_9$ is a metastable phase, which decomposes gradually into $Al_{18}B_4O_{33}$ and B_2O_3 up to 1000 °C, and the latter

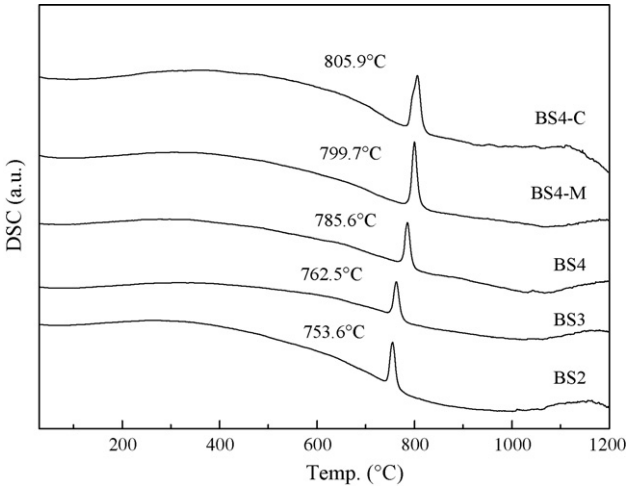

Fig. 2. DSC curves of the glass samples at heating rate of 10 °C min^{-1}.

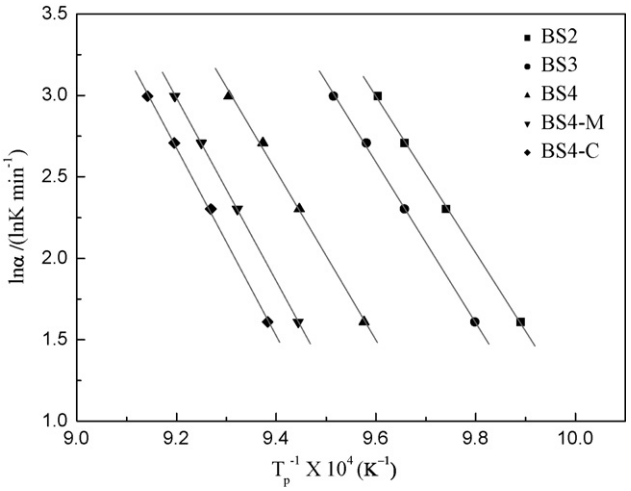

Fig. 3. Plots of $\ln\alpha$ vs. $1/T_p$ for the glass samples.

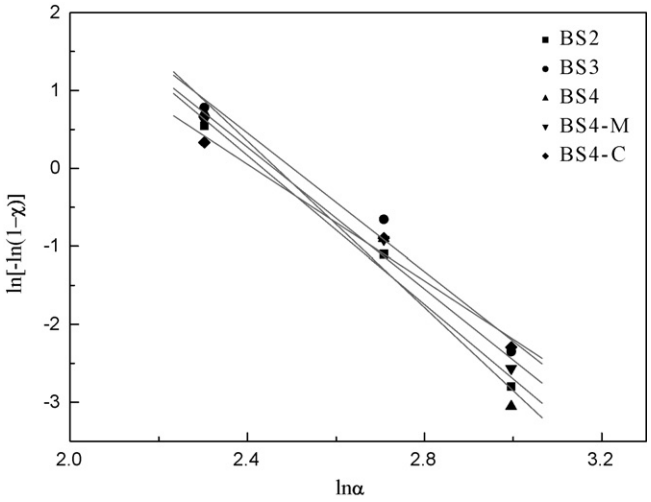

Fig. 4. Plots of $\ln[-\ln(1-x)]$ vs. $\ln\alpha$ for the glass samples.

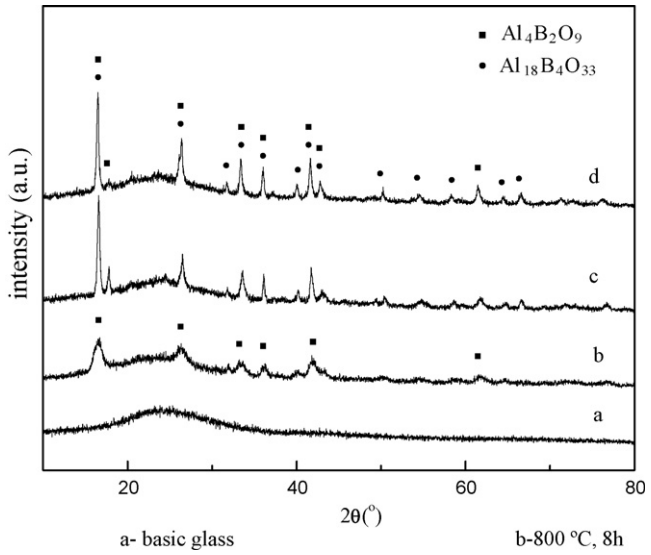

Fig. 5. XRD patterns of BS3 heat-treated at different temperatures.

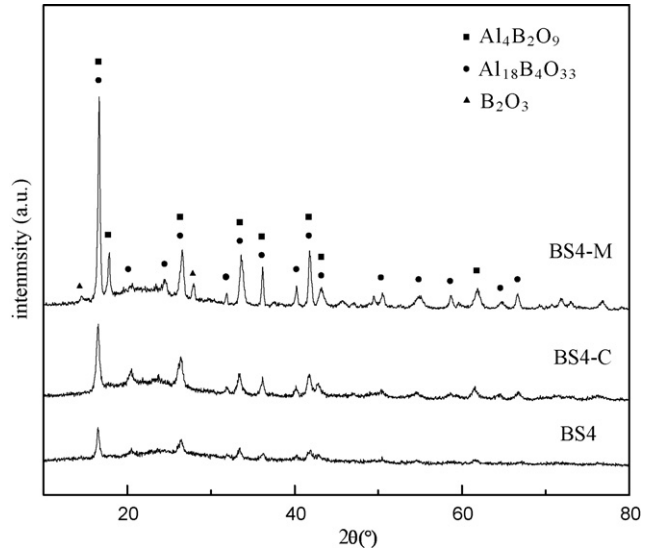

Fig. 6. XRD patterns of BS4, BS4-M and BS4-C heat-treated at 1100 °C for 2 h.

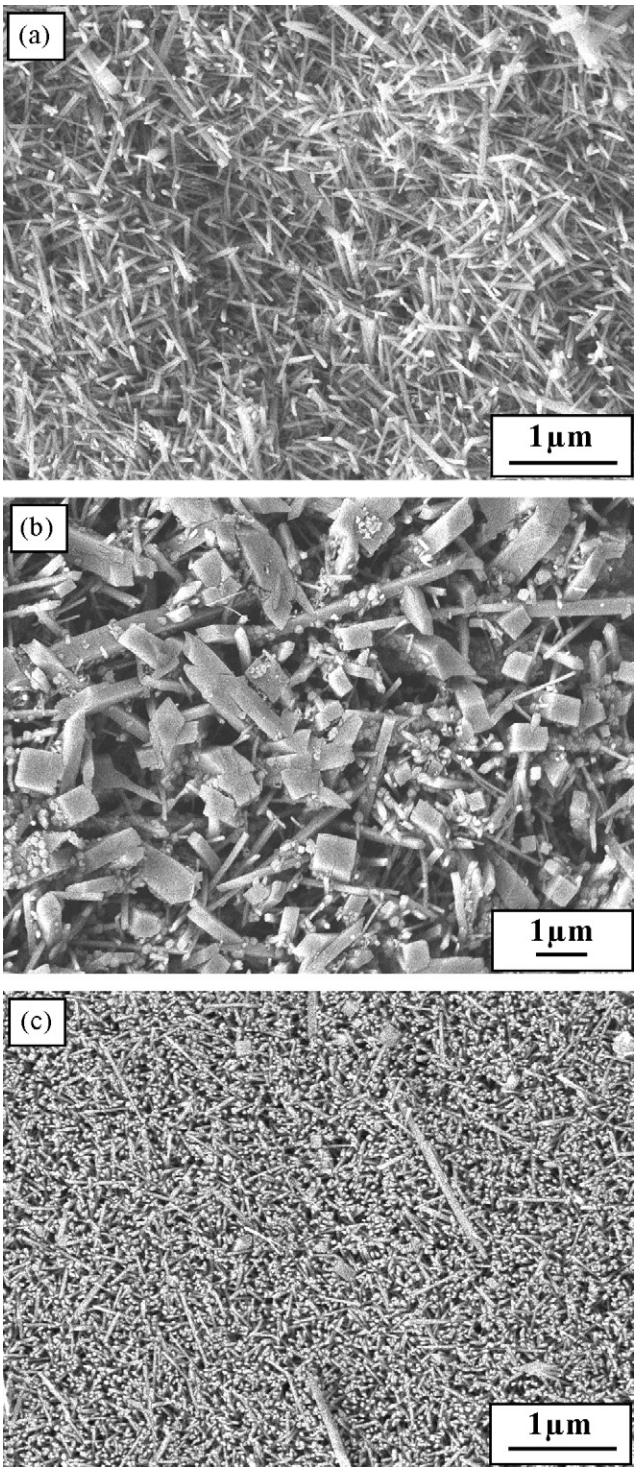

Fig. 7. SEM micrographs of samples heat-treated at 1100 °C for 2 h, (a) BS4, (b) BS4-M, (c) BS4-C.

evaporated slowly. $Al_{18}B_4O_{33}$ is a stable phase at least up to 1200 °C. The possible reactions in the process are:

$$2Al_2O_3 + B_2O_3 = Al_4B_2O_9 \quad (8)$$

$$9Al_4B_2O_9 = 2Al_{18}B_4O_{33} + 5B_2O_3\uparrow \quad (9)$$

$$9Al_2O_3 + 2B_2O_3 = Al_{18}B_4O_{33} \quad (10)$$

Table 5
Thermal expansion coefficient and soften temperature of glass-ceramic samples

Sample	Thermal expansion coefficient ($\times 10^{-6}$/°C)	Soften temperature (°C)
BS4	5.216	1184.3
BS4-M	5.188	1175.4
BS4-C	5.674	1180.7

The scanning electron microscopy (SEM) micrographs of the polished and etched surface of BS4, BS4-M and BS4-C heat-treated at 1100 °C for 2 h are shown in Fig. 7. It can be clearly observed that the bulk crystallization in the three samples, and the morphology of crystals in sample BS4 and BS4-C are needle like crystals about 1–2 μm in length and 0.1 μm in diameter, while the sample BS4-M is square columnar crystals about 5–6 μm in length and 0.8 μm in section length. The addition of different alkali earth metal oxides to B_2O_3–Al_2O_3–SiO_2 system has evident effects not only on the main crystalline phase, but also on the morphology of the crystals.

The thermal expansion coefficient and the soften temperature of heat-treated samples are listed in Table 5. The value of BS4-M specimen is lower than the other two. The lower thermal expansion coefficient and higher soften temperatures of B_2O_3–Al_2O_3–SiO_2 glass-ceramics make it important for the applications in electronical purposes.

5. Conclusions

MO (M=Ba, Mg, Ca) can improve the glass formation of B_2O_3–Al_2O_3–SiO_2 system, and which is affected by the ratio of B_2O_3/SiO_2. For the addition of BaO in the glasses, the feasible B_2O_3/SiO_2 ratio is between 1.0 and 1.6. The crystallization capacity of the glass decreases with the reduction of B_2O_3/SiO_2 ratio. The predominating crystal phase is $Al_4B_2O_9$ when heat-treated at 800 °C, which could transfer into $Al_{18}B_4O_{33}$ slowly when the temperature rises up to 1100 °C. The activation energy E shows the order of the crystallization capacity of the glass-ceramics to be CaO < MgO < BaO. The Avrami exponent n indicates that the crystallization mechanism of B_2O_3–Al_2O_3–SiO_2 system is attributed by bulk nucleation with three-dimensional crystal growth.

References

[1] X. Liu, Y. Wang, Some characteristics of glass in the Al_2O_3–B_2O_3–SiO_2 system from the gel, J. Non-Cryst. Solids 80 (1986) 564–570.
[2] P.J. Vergano, US 3 997 351 (18 June 1975).
[3] E. M.A. Hamzawy, A.F. Ali, Sol–gel synthesis and crystallization of aluminum borosilicate, Ceram. Int. 27 (2001) 607–613.
[4] R. Zheng, S.R. Wang, H.W. Nie, T.-L. Wen, SiO_2–CaO–B_2O_3–Al_2O_3 ceramic glaze as sealant for planar ITSOFC, J. Power Sources 128 (2004) 165–172.
[5] P.W. Micmillan, Glass Ceramic, 2nd ed., Academic Press, London, 1979.
[6] H. Yinnon, D.R. Uhlmann, Application of thermoanalytical techniques to the study of crystallization kinetics in glass-forming liquids. Part I. Theory, J. Non-Cryst. Solids 54 (1983) 253–275.
[7] J. Zhu, Z. Bo, D. Dong, Crystallization kinetics of InF_3 based glass by differential scanning calorimetry, J. Non-Cryst. Solids 201 (1996) 47–51.
[8] H. Shao, K. Liang, F. Peng, Crystallization kinetics of MgO–Al_2O_3–SiO_2 glass-ceramics, Ceram. Int. 30 (2004) 927–930.
[9] C.S. Ray, W.H. Huang, D.E. Day, Crystallization kinetics of a lithia-silica glass: effect of sample characteristics and thermal analysis measurement techniques, J. Am. Ceram. Soc. 74 (1991) 60–66.
[10] R. Iordanova, E. Lefterova, I. Uzunov, D. Klissurshi, Non-isothermal crystallization kinetics of V_2O_5–MoO_3–Bi_2O_3 glasses, J. Therm. Anal. Calorm. 70 (2002) 393–404.
[11] Y. Cheng, H. Xiao, W. Guo, W. Guo, Structure and crystallization kinetics of PbO–B_2O_3 glasses, Ceram. Int. 33 (2007) 1341–1347.
[12] Y. Cheng, H. Xiao, W. Guo, W. Guo, Structure and crystallization kinetics of Bi_2O_3–B_2O_3 glasses, Thermochim. Acta 444 (2006) 173–178.
[13] C. Dayanand, M. Salagram, Thermal (DSC) characterization of xPbO–$(1-x)P_2O_5$ glass system, Ceram. Int. 30 (2004) 1731–1735.
[14] T. Ozawa, Kinetic of non-isothermal crystallization, Polymer 12 (1971) 150–158.
[15] D. Mazza, M. Vallino, G. Busca, Mullite-type structures in the systems Al_2O_3–Me_2O (Me = Na, K) and Al_2O_3–B_2O_3, J. Am. Ceram. Soc. 75 (1992) 1929–1934.
[16] G. Werding, W. Schreyer, Synthsis and stability of werdingite, a new phase in the system MgO–Al_2O_3–B_2O_3–SiO_2 (MABS),and another new phase in the ABS-system, Eur. J. Mineral. 4 (1992) 193–207.